TOC

Renewable micro-mesoporous carbons show enhanced ability to store both H_2 and CO_2 at high pressure (≥ 20 bar).

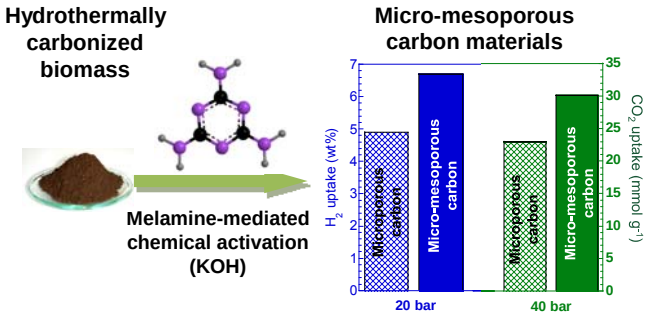

Highly porous renewable carbons for enhanced storage of energy-related gases (H_2 and CO_2) at high pressures

Marta Sevilla,[a,*] Wantana Sangchoom,[b] Norah Balahmar,[b] Antonio B. Fuertes,[a] R. Mokaya[b,*]

[a] Instituto Nacional del Carbón (CSIC), P.O. Box 73, Oviedo 33080, Spain
[b] School of Chemistry, University of Nottingham, University Park, NG7 2RD Nottingham, UK.

[*] Corresponding author: martasev@incar.csic.es (M. Sevilla); r.mokaya@nottingham.ac.uk (R. Mokaya)

Abstract

Hydrochar, *i.e.,* hydrothermally carbonized biomass, is generating a great interest as precursor for the synthesis of advanced carbon materials owing to economical, sustainability and availability issues. Hereby its versatility to produce adsorbents with a porosity adjusted to the targeted application, *i.e.*, low or high pressure gas adsorption applications is shown. Such tailoring of the porosity is achieved through the addition of melamine to the mixture hydrochar/KOH used in the activation process. Thereby, high surface area carbons (> 3200 m^2 g^{-1}) with a bimodal porosity in the micro-mesopore range are obtained, whereas conventional KOH chemical activation leads to microporous materials (surface area < 3100 m^2 g^{-1}). The micro-mesoporous materials thus synthesized show enhanced ability to store both H_2 and CO_2 at

high pressure (≥ 20 bar). Indeed, the uptake capacities recorded at 20 bar, *ca.* 7 wt % H_2 (-196 ºC) and 19-21 mmol CO_2 g^{-1} (25 ºC), are among the highest ever reported for porous materials. Furthermore, the micro-mesoporous sorbents are far from saturation at 20 bar, and achieve much higher CO_2 uptake at 40 bar (up to 31 mmol CO_2 g^{-1}) (25 ºC) compared to 23 mmol CO_2 g^{-1} for the microporous materials. In addition, the micro-mesoporous materials show enhanced working capacities since the abundant mesoporosity ensures higher capture at high uptake pressure and the retention of lower amounts of adsorbed gas at the regeneration pressure used in PSA systems.

Keywords: mesoporosity, hydrogen, carbon dioxide, hydrothermal carbonization, chemical activation, melamine

Introduction

The development of porous carbon materials combining an appropriate pore size distribution with large surface areas has proven to very challenging. Such carbon materials are required in order to achieve advancement in many clean energy technologies, such as fuel cells (*i.e.,* hydrogen storage and electrocatalysts),[1, 2] carbon capture,[3, 4] and electrochemical energy storage in supercapacitors or batteries. [5-8] Furthermore, in order to assess a material development as being sustainable, the synthesis and fabrication methods should rely on efficient, safe and environmentally sound preparation schemes. Consequently, intensive research efforts are currently being directed towards the development of novel synthesis procedures for the production of porous carbon materials. We and others have shown, for example, that by the simple heat-treatment of appropriate organic salts, highly porous carbon materials can be obtained.[9-14] _ENREF_1 However, the porosity of such materials is either usually limited to being within the micropore range[14-16] or is low,[12, 13] which hampers their utilization in some specific applications. Thus, for the storage of energy-related gases, *i.e.*, H_2 and CO_2, at high pressure, which is essential for attainment of the anticipated Hydrogen Economy, whilst some studies show that narrow micropores are the most effective pores, larger micropores and small mesopores also contribute to the adsorption process, with the storage capacity showing a positive correlation with the surface area.[17, 18] Chemical activation of carbon precursors with KOH has increasingly attracted interest as a simple and efficient method for fabricating porous carbons with very high specific surface area (> 2000m^2 g^{-1}). [19-21] However, the porosity of KOH activated carbons is

normally within the micropore range with the proportion of mesoporosity being very low.[19, 22, 23] Only a limited number of precursors are able to give rise to activated materials with a high proportion of small mesopores in addition to micropores *via* KOH activation, such as zeolite-templated carbons,[24] polypyrrole,[18] graphene[25] or ionic liquid-derived carbon.[26] From a sustainable and availability standpoint biomass is a more desirable precursor. However, due to the heterogeneity and low carbon yield of biomass precursors, there have been recent moves toward the use of so-called hydrochar*, i.e.,* hydrothermally carbonized biomass, as a more appropriate precursor.[27] The above considerations with respect to sustainable synthesis of micro-mesoporous activated carbon have motivated us to explore activation procedures capable of generating highly porous carbons with a bimodal porosity in the micro-mesopore range from hydrochar. Accordingly, herein we present a melamine-mediated KOH chemical activation procedure for the synthesis of hydrochar-derived high surface area carbons with bimodal porosity that combines narrow micropores (*ca.* 1 nm) and small mesopores (2-5 nm). Analysis of their ability to store H_2 (-196 ºC) and CO_2 (25 ºC) at high pressure (≥ 20 bar) gave values (*ca.* 7 wt % H_2 and 19-21 mmol CO_2 g^{-1} at 20 bar, and up to 31 mmol CO_2 g^{-1} at 40 bar) which are among the highest ever reported for porous materials as a result of their optimum pore characteristics.

Experimental section

Synthesis of porous carbon materials

Hydrochar products were prepared by the hydrothermal carbonization of potato starch (Aldrich), cellulose (Aldrich) and eucalyptus sawdust (Local sawmill). Briefly, an aqueous solution/dispersion of the raw material (concentration: 320 $g \cdot L^{-1}$) was placed in a stainless steel autoclave, heated up to 250 ºC and kept at this temperature for 2 h. The resulting carbonaceous solid, denoted as *hydrochar*, was recovered by filtration, washed with distilled water and dried at 120 ºC over a period of several hours.

The hydrochar materials were chemically activated using potassium hydroxide (Sigma-Aldrich) in the presence of melamine (Aldrich). Briefly, a *hydrochar* sample was thoroughly ground with KOH (KOH/*Hydrochar* weight ratio of 4) and melamine (Melamine/*Hydrochar* weight ratio of 2 or 3). Subsequently, the mixture was heat-treated up to 800 ºC (heating rate: 3 $ºC \cdot min^{-1}$) under a nitrogen gas flow and held at this temperature for 1 h. The samples were then thoroughly washed several times with 10 wt% HCl to remove any inorganic salts, washed with distilled water until a neutral pH was obtained and finally dried in an oven at 120 ºC for 3 h. The activated carbons thus synthesized were denoted as *AX–yM*, where *X* refers to the raw material (*A*: starch, *C*: cellulose and *S*: sawdust) and *y* = 2 or 3 (*i.e.* Melamine/Hydrochar weight ratio). Porous carbons were also produced in the absence of melamine by simple activation of the hydrochar materials with KOH (KOH/Hydrochar weight ratio = 4) at a temperature of 800 ºC. These samples were denoted as A*X*–0.

Characterization

The nitrogen sorption isotherms of the carbon samples were measured at −196 °C using a Micromeritics ASAP 2020 sorptometer. The apparent surface area

(S_{BET}) was calculated from the N_2 isotherms using the Brunauer-Emmett-Teller (BET) method. An appropriate relative pressure range was selected to ensure that a positive line intersect of multipoint BET fitting (C > 0) would be obtained and $V_{ads}(1 - p/p_o)$ would increase with p/p_o.[28, 29] The total pore volume (V_p) was determined from the amount of nitrogen adsorbed at a relative pressure (p/p_o) of 0.95. The micropore volume (V_m) was obtained by applying the Dubinin-Radushkevich equation.[30] The micropore size distributions were determined by means of the quenched-solid density functional theory (QSDFT) method applied to the nitrogen adsorption data and assuming a slit pore model. Scanning electron microscopy (SEM) images were obtained on a Quanta FEG650 (FEI) instrument. X-ray photoelectron spectroscopy (XPS) was carried out on a Specs spectrometer, using Mg K α (1253.6 eV) radiation from a double anode at 50 w. Binding energies for the high resolution spectra were calibrated by setting C 1s to 284.6 eV. Elemental analysis (C, N and O) of the samples was carried out on a LECO CHN-932 microanalyzer.

Gas uptake measurements

Hydrogen (high purity, 99.9999%) uptake measurements were performed over the pressure range of 0-20 bar with an Intelligent Gravimetric Analyzer (IGA-003 Hiden). Before analysis, the samples were outgassed under vacuum at 200 °C overnight. Then the hydrogen uptake isotherms were measured at −196 °C (under a liquid nitrogen bath). The hydrogen uptake was corrected for buoyancy effect as previously described.[31] CO_2 uptake isotherms at 25 ºC were obtained over the pressure range of 0-40 bar with a XEMIS Intelligent Gravimetric Analyzer. The samples were outgassed at 200 ^oC overnight before analysis.

Heats of adsorption were measured in a calorimeter Setaram C80 connected to an adsorption equipment Quantachrome's Autosorb AS-1.

Results and discussion

Scheme 1 illustrates the synthesis methodology followed for the production of highly micro-mesoporous carbon materials from biomass-derived hydrochars, using both simple (cellulose and starch) and more complex (sawdust) biomass products. This procedure is based on a melamine-mediated chemical activation process, using KOH as chemical activating agent wherein melamine plays a dual role as: a) structure-directing agent thus extending the pore size distribution into the mesopore region and b) N-dopant. Indeed, as exemplified in Figures 1a and1b for starch- and sawdust-derived hydrochars respectively, the shape of the isotherm is transformed from type I, typical of microporous materials (sample AA-0 and AS-0) to one exhibiting both type I and IV characteristics attributable to materials combining both micropores and small mesopores, when melamine is incorporated into the activation mixture (samples AA-2M, AA-3M, AS-2M and AS-3M). This is further corroborated by the pore size distributions (PSDs) in Figures 1c and 1d. Thus, although both sets of samples exhibit a bimodal PSD, the pore size range of samples AA-0 and AS-0 is exclusively centered in the micropore region with narrow micropores at 0.85 nm and supermicropores at ~ 1.5 nm, whereas for samples AA-2M, AA-3M, AS-2M and AS-3M the pore size range extends into the mesopore range (up to ~4-5 nm), with a maximum at ~ 2.2 nm, in addition to the narrow micropores at 0.85 nm. Similar trends in pore size are obtained for cellulose-derived carbons

(Figure S1), or for simple monosaccharides such as glucose as we have recently shown,[32] which suggests the general validity of this methodology for hydrochar. As can be seen in the high-resolution transmission electron microscopy (HRTEM) images in Figure S2, the pores of these carbons are randomly distributed as is typical for such highly activated carbons, and are of varying pore size within the micropore and low mesopore range in agreement with the N_2 sorption PSDs. Furthermore, large magnifications of the HRTEM images evidence that AS-2M possesses larger mesopores than AS-0, also in accordance with the PSDs. The textural properties of the activated carbons from a variety of hydrochar mixes are summarized in Table 1. As can be seen, the activated carbons produced through the melamine-mediated chemical activation process exhibit ultra-high BET surface areas, in the ~3000-3500 $m^2 g^{-1}$ range and pore volumes of 2.2-2.4 $cm^3 g^{-1}$, values that are double those (*i.e.* ~1.0-1.46 $cm^3 g^{-1}$) of the analogous materials produced through conventional chemical activation.[19] Importantly, the porosity of the present micro-mesoporous materials is almost equally distributed between micropores and mesopores (V_{micro}/V_{meso} ratio ~ 0.8-1.4), whereas the materials produced through conventional chemical activation are essentially microporous with the mesopore volume representing less than 25% of the total pore volume (Table 1). Interestingly, increase of the melamine/hydrochar ratio from 2 (AA-2M) to 3 (AA-3M) has no significant effect on the PSD, as shown in Figures 1b and 1d. However, it does lead to a substantial increase in the N content of the samples. Thus, materials synthesized using a melamine/hydrochar ratio of 2 possess a nitrogen content of 1.3-1.7 wt%, whereas those synthesized with a melamine/hydrochar ratio of 3 exhibit a nitrogen content higher than 3 wt%

(Table S1). Elemental energy-dispersive X-ray (EDX) mapping images of the materials prove that the nitrogen heteroatoms are uniformly distributed within the N-doped particles (Figure S3). On the other hand, X-ray photoelectron spectroscopy (XPS) shows that the nitrogen heteroatoms exist in a variety of moieties: i) pyridinic-N at 398.2-398.3 eV, ii) pyrrolic-/pyridonic-N at 400.1-400.2 eV and iii) pyridine N-oxide 402.2-402.3 eV (Figure S4). As we have previously described in detail, N-doping by melamine takes place through the decomposition of the carbon nitride (*g*-C_3N_4) formed from the polymerization of melamine at T > 550 ºC. [33] Taking into account that a decrease in activated carbon yield is registered when melamine is added to the KOH/hydrochar mixture (*e.g.* from 23% for AS-0 to 18% for AS-2M), we believe that the gases generated in the decomposition of melamine gasify part of the carbon causing enlargement of pore size in parallel with the incorporation of nitrogen atoms into the carbon framework.

Given the textural properties of these materials, *i.e.*, large surface area and pore volume arising from micropores and small mesopores, we assessed their high pressure H_2 storage and CO_2 adsorption capability. AA-3M, AC-2M and AS-2M were selected for this study. Accordingly, Figure 2 shows the total H_2 uptake isotherms at -196 ºC over the pressure range of 0-20 bar and Figure 3 the total CO_2 uptake isotherms at 25 ºC over the pressure range of 0-40 bar, while Table 2 summarizes the H_2 and CO_2 uptake capacities at 20 bar and CO_2 uptake at 40 bar. As can be seen in Figure 2 and Table 2, all the micro-mesoporous materials exhibit large H_2 uptakes, both for excess (≥ 5 wt% equivalent to ≥ 25 mmol g^{-1}) and total (> 6 wt% equivalent to 30 mmol g^{-1}) storage capacity. Furthermore, no saturation is observed at 20 bar for the total

H_2 isotherms, implying that greater hydrogen storage could be achieved at higher pressure. Indeed, the maximum total hydrogen uptake estimated *via* fitting of the up to 20 bar data using the Langmuir model[34, 35] ENREF 9 is in the 7.9-8.2 wt% (equivalent to 39.5-41 mmol g^{-1}) range. The total H_2 uptake at 20 bar of the materials here developed, *i.e.,* 6.4-6.8 wt% (equivalent to 32-34 mmol g^{-1}), is comparable to the best performing carbons reported in the literature (Table S2). On the other hand, when compared to the microporous carbons AA-0 and AC-0 (see Table 2 and Figure 2), a *ca.* 30-40% enhancement in the amount of hydrogen stored is recorded (the enhancement being greater for the estimated maximum hydrogen uptake), thus confirming that small mesopores can positively contribute to hydrogen adsorption at high pressure. In this regard, as shown in Figures S5a-b, good correlations (with a y-axis intersection of approximately zero) are obtained between the hydrogen uptake at 20 bar and the volume of pores < 3 nm (determined through the QSDFT method), and the estimated maximum hydrogen uptake and the total pore volume. In addition, the hydrogen uptake of the present micro-mesoporous carbons is in line with the Chahine rule, which stipulates an uptake of 10 μmol H_2 m^{-2} (Figure S5c). These findings are very similar to those we have previously obtained with N-doped micro-mesoporous carbons synthesized by chemical activation of polypyrrole (Figure S5c),[18] which is not surprising given the similarity in their textural characteristics. However, the present carbon materials have the environmental and economic advantages of being synthesized from biomass.

The CO_2 capture capacity of the micro-mesoporous carbon materials was assessed at high pressure and ambient temperature, *i.e.*, under conditions relevant to pre-combustion CO_2 capture using pressure swing adsorption (PSA)

systems. As can be seen in Figure 3 and Table 2, the micro-mesoporous carbons exhibit large CO_2 uptakes at 20 bar, in the 20-21 mmol CO_2 g^{-1} range (~ 88-93 wt% CO_2). These values are amongst the highest ever reported for porous carbon materials or metal-organic frameworks as can be deduced from the data in Table 3. On the other hand, the uptake values are very similar to those for the microporous materials, *i.e.* ~19.5 mmol CO_2 g^{-1} (Table 2). This result suggests that 20 bar is not high enough pressure to fill the small mesopores. Indeed, as revealed by Figure 3, and summarized in Table 2, increase of the pressure up to 40 bar yields large uptake capacities of 30-31 mmol CO_2 g^{-1} in the case of the micro-mesoporous carbons, in contrast to *ca.* 23.5 mmol CO_2 g^{-1} for the microporous carbons (*i.e.* a 30 % enhancement in uptake capacity at 40 bar *vs.* < 10 % enhancement at 20 bar). More generally, the high pressure ($\geq$ 20 bar) CO_2 uptake of the present micro-mesoporous materials surpasses that of benchmark porous carbons that are mainly microporous as shown in Table 3. In this regard, Figure 3 clearly shows the influence of porosity (*i.e.* micro- or mesoporosity) on CO_2 uptake. Thus, for pressures lower than ~ 13 bar, the materials with a microporous nature and abundant narrow microporosity (Figures 1c, 1d and S1b) adsorb the most owing to the enhanced adsorption potential in such pores,[36] whereas for higher pressures the micro-mesoporous materials surpass the microporous ones. More importantly, as mesopores are being progressively filled with the rise of pressure and micropores saturate, the difference in uptake capacity between the micro-mesoporous and the microporous carbons steadily increases (see arrows in Figure 3). This is a clear advantage for PSA systems. In this regard, simulation of the CO_2 isotherm at 25 ºC up to 100 bar using a Langmuir model

(see Figure S6) evidences that much larger uptakes could still be achieved for the micro-mesoporous carbons by increasing further the pressure, contrarily to the microporous carbons.

Even though the uptake capacity can be used as preliminary parameter to screen out CO_2 sorbents, a more relevant parameter when using a PSA system for CO_2 capture is the working capacity which takes into account the adsorption and desorption (regeneration) pressures. Considering 20 bar and atmospheric pressure respectively as the adsorption and desorption pressures, the working capacity of the micro-mesoporous sorbents is ~ 18 mmol CO_2 g^{-1}, increasing to ~ 28 mmol CO_2 g^{-1} for an adsorption pressure of 40 bar and desorption at 1 bar (Table 2). Both values of working capacity are superior to those of many benchmark porous carbons and MOFs (Table 3). Importantly, the working capacity of the micro-mesoporous carbons is much higher than that of the microporous materials. In fact, the difference in working capacity between the two sets of samples (being *ca.* 40 % higher for the micro-mesoporous samples) is larger than the 30 % enhancement in uptake capacity (at 40 bar). This is due to the fact that the adsorption capacity at 1 bar of the microporous carbons is greater, as shown in Table 2 (and Figure S7a), which means that they retain higher amounts of CO_2 at the desorption pressure of 1 bar. This result correlates well with the abundant narrow microporosity in the microporous carbons, which enhances CO_2 adsorption at low pressures.[36, 37] This is further corroborated by comparison of the heat of adsorption of AC-0 (~19-21 kJ mol^{-1}) and AC-2M (~16-19 kJ mol^{-1}) (see Figure S7b). Therefore, the presence of abundant mesoporosity in a sorbent is not only important for achieving high adsorption capacity at high pressures, but for ensuring low amounts of CO_2

remaining in the sorbent after the regeneration process. Overall, these results show that it is very important to tune the pore structure of the adsorbent depending on the targeted application, *i.e.* low (post-combustion) or high pressure (pre-combustion) adsorption. In these regard, hydrochar is a very versatile precursor, as materials with a large volume of narrow micropores can be generated through conventional KOH chemical activation by controlling the KOH/hydrochar ratio and activation temperature,[37] whereas materials containing narrow micropores and small mesopores can be synthesized by a melamine-mediated KOH chemical activation process.

Conclusions

In summary, hydrochar-based high surface area carbons with bimodal porosity in the micro-mesopore range have been prepared via a melamine-mediated KOH chemical activation process by using both simple (starch, cellulose) and complex (sawdust) biomass. The micro-mesoporous materials show enhanced ability to store both H_2 and CO_2 at high pressure (≥ 20 bar) owing to the right combination of narrow micropores and small mesopores. Importantly, at 20 bar the sorbents are far from saturation, which indicates that much larger uptakes can be achieved at higher pressure. Moreover, the abundant mesoporosity ensures the retention of low amounts of adsorbed gas at regeneration pressures typically used in PSA systems, which translates to enhanced working capacities. The uptake capacities recorded at 20 bar, *ca.* 7 wt % H_2 (-196 ºC) and 19-21 mmol CO_2 g^{-1} (25 ºC), and up to 31 mmol CO_2 g^{-1} at 40 bar (and 25 ºC) are amongst the highest ever reported for porous materials.

Acknowledgements

This research work was supported by Spanish Ministerio de Economía y Competitividad, MINECO (MAT2012-31651), and by Fondo Europeo de Desarrollo Regional (FEDER). M. S. thanks the Ministerio de Ciencia e Innovación for her Ramón y Cajal contract. We thank the Rajamangala University of Technology Srivijaya (RMUTSV), Thailand for funding and a studentship for WS, and the Kingdom of Saudi Arabia for funding a PhD studentship for NB.

ASSOCIATED CONTENT

Supporting Information

Tables gathering the chemical composition of the porous carbons and comparing the H_2 storage capacity of the porous carbons with those of other materials that can be found in the literature; figures containing isotherms, pore size distributions, HRTEM, SEM-EDX, XPS spectra, correlations of H_2 uptake and textural parameters, simulation of high pressure CO_2 adsorption isotherms, CO_2 adsorption isotherms at low pressure and CO_2 heats of adsorption. This material is available free of charge via the Internet at http://pubs.acs.org.

References

1. Xia, Y.; Yang, Z.; Zhu, Y. Porous carbon-based materials for hydrogen storage: advancement and challenges. *J. Mater. Chem. A* **2013**, *1*, 9365-9381.
2. Tang, J.; Liu, J.; Torad, N. L.; Kimura, T.; Yamauchi, Y. Tailored design of functional nanoporous carbon materials toward fuel cell applications. *Nano Today* **2014**, *9*, 305-323.
3. Balahmar, N.; Mitchell, A. C.; Mokaya, R. Generalized Mechanochemical Synthesis of Biomass-Derived Sustainable Carbons for High Performance CO2 Storage. *Adv. Energy Mater.* **2015**, *5*, n/a-n/a.
4. Presser, V.; McDonough, J.; Yeon, S. H.; Gogotsi, Y. Effect of pore size on carbon dioxide sorption by carbide derived carbon. *Energy Environ. Sci.* **2011**, *4*, 3059-3066.

5. Béguin, F.; Presser, V.; Balducci, A.; Frackowiak, E. Carbons and Electrolytes for Advanced Supercapacitors. *Adv. Mater.* **2014**, *26*, 2219-2251.
6. Borchardt, L.; Oschatz, M.; Kaskel, S. Tailoring porosity in carbon materials for supercapacitor applications. *Materials Horizons* **2014**, *1*, 157-168.
7. Manthiram, A.; Chung, S.-H.; Zu, C. Lithium–Sulfur Batteries: Progress and Prospects. *Adv. Mater.* **2015**, *27*, 1980-2006.
8. Zhang, K.; Hu, Z.; Chen, J. Functional porous carbon-based composite electrode materials for lithium secondary batteries. *Journal of Energy Chemistry* **2013**, *22*, 214-225.
9. Atkinson, J. D.; Rood, M. J. Preparing microporous carbon from solid organic salt precursors using in situ templating and a fixed-bed reactor. *Microp. Mesop. Mater.* **2012**, *160*, 174-181.
10. Sevilla, M.; Fuertes, A. B. A general and facile synthesis strategy towards highly porous carbons: carbonization of organic salts. *J. Mater. Chem. A* **2013**, *1*, 13738-13741.
11. Luo, H.; Yang, Y.; Zhao, X.; Zhang, J.; Chen, Y. 3D sponge-like nanoporous carbons via a facile synthesis for high-performance supercapacitors: direct carbonization of tartrate salt. *Electrochim. Acta* **2015**, *169*, 13-21.
12. Ferrero, G. A.; Sevilla, M.; Fuertes, A. B. Mesoporous carbons synthesized by direct carbonization of citrate salts for use as high-performance capacitors. *Carbon* **2015**, *88*, 239-251.
13. Fuertes, A. B.; Sevilla, M. Hierarchical Microporous/Mesoporous Carbon Nanosheets for High-Performance Supercapacitors. *ACS App. Mater. Interfases* **2015**, *7*, 4344-4353.
14. Puthusseri, D.; Aravindan, V.; Madhavi, S.; Ogale, S. 3D micro-porous conducting carbon beehive by single step polymer carbonization for high performance supercapacitors: the magic of in situ porogen formation. *Energy Environ. Sci.* **2014**, *7*, 728-735.
15. Sevilla, M.; Fuertes, A. B. Direct Synthesis of Highly Porous Interconnected Carbon Nanosheets and Their Application as High-Performance Supercapacitors. *ACS Nano* **2014**, *8*, 5069-5078.
16. Adeniran, B.; Masika, E.; Mokaya, R. A family of microporous carbons prepared via a simple metal salt carbonization route with high selectivity for exceptional gravimetric and volumetric post-combustion CO2 capture. *J. Mater. Chem. A* **2014**, *2*, 14696-14710.
17. Casco, M. E.; Martínez-Escandell, M.; Silvestre-Albero, J.; Rodríguez-Reinoso, F. Effect of the porous structure in carbon materials for CO2 capture at atmospheric and high-pressure. *Carbon* **2014**, *67*, 230-235.
18. Sevilla, M.; Mokaya, R.; Fuertes, A. B. Ultrahigh surface area polypyrrole-based carbons with superior performance for hydrogen storage. *Energy Environ. Sci.* **2011**, *4*, 2930-2936.
19. Sevilla, M.; Mokaya, R. Energy storage applications of activated carbons: supercapacitors and hydrogen storage. *Energy Environ. Sci.* **2014**, *7*, 1250-1280.
20. Sevilla, M.; Mokaya, R. Activation of carbide-derived carbons: a route to materials with enhanced gas and energy storage properties. *J. Mater. Chem.* **2011**, *21*, 4727-4732.
21. Wang, J.; Kaskel, S. KOH activation of carbon-based materials for energy storage. *J. Mater. Chem.* **2012**, *22*, 23710-23725.
22. Kierzek, K.; Frackowiak, E.; Lota, G.; Gryglewicz, G.; Machnikowski, J. Electrochemical capacitors based on highly porous carbons prepared by KOH activation. *Electrochim. Acta* **2004**, *49*, 515-523.
23. Maciá-Agulló, J. A.; Moore, B. C.; Cazorla-Amorós, D.; Linares-Solano, A. Activation of coal tar pitch carbon fibres: Physical activation vs. chemical activation. *Carbon* **2004**, *42*, 1367-1370.
24. Sevilla, M.; Alam, N.; Mokaya, R. Enhancement of hydrogen storage capacity of zeolite-templated carbons by chemical activation. *J. Phys. Chem. C* **2010**, *114*, 11314-11319.
25. Zhu, Y.; Murali, S.; Stoller, M. D.; Ganesh, K. J.; Cai, W.; Ferreira, P. J.; Pirkle, A.; Wallace, R. M.; Cychosz, K. A.; Thommes, M.; Su, D.; Stach, E. A.; Ruoff, R. S. Carbon-Based Supercapacitors Produced by Activation of Graphene. *Science* **2011**, *332*, 1537-1541.

26. Kim, M.-H.; Yun, S.; Park, H. S.; Han, J. T.; Kim, K.-B.; Roh, K. C. Retransformed graphitic activated carbon from ionic liquid-derived carbon containing nitrogen. *J. Mater. Chem. A* **2015**, *3*, 2564-2567.
27. Sevilla, M.; Falco, C.; Titirici, M.-M.; Fuertes, A. B. High-performance CO2 sorbents from algae. *RSC Adv.* **2012**, *2*, 12792-12797.
28. *ISO 9277:2010. Determination of the specific surface area of solids by gas adsorption - BET method. Second Edition of ISO 9277, ISO*; Geneva, **2012**.
29. Rouquerol, F.; Rouquerol, J.; Sing, K. *Adsorption by powders and porous solids: principles, methodology and applications*. Academic Press: San Diego **1999**.
30. Dubinin, M. M. Fundamentals of the theory of adsorption in micropores of carbon adsorbents: Characteristics of their adsorption properties and microporous structures. *Carbon* **1989**, *27*, 457-467.
31. Yang, Z.; Xia, Y.; Mokaya, R. Enhanced Hydrogen Storage Capacity of High Surface Area Zeolite-like Carbon Materials. *J. Am. Chem. Soc.* **2007**, *129*, 1673-1679.
32. Fuertes, A. B.; Sevilla, M. Superior Capacitive Performance of Hydrochar-Based Porous Carbons in Aqueous Electrolytes. *ChemSusChem* **2015**, *8*, 1049-1057.
33. Fuertes, A. B.; Ferrero, G. A.; Sevilla, M. One-pot synthesis of microporous carbons highly enriched in nitrogen and their electrochemical performance. *J. Mater. Chem. A* **2014**, *2*, 14439-14448.
34. Zheng, Z.; Gao, Q.; Jiang, J. High hydrogen uptake capacity of mesoporous nitrogen-doped carbons activated using potassium hydroxide. *Carbon* **2010**, *48*, 2968-2973.
35. Masika, E.; Mokaya, R. Exceptional gravimetric and volumetric hydrogen storage for densified zeolite templated carbons with high mechanical stability. *Energy Environ. Sci.* **2014**, *7*, 427-434.
36. Sevilla, M.; Parra, J. B.; Fuertes, A. B. Assessment of the Role of Micropore Size and N-Doping in CO2 Capture by Porous Carbons. *ACS App. Mater. Interfases* **2013**, *5*, 6360-6368.
37. Sevilla, M.; Fuertes, A. B. Sustainable porous carbons with a superior performance for CO2 capture. *Energy Environ. Sci.* **2011**, *4*, 1765-1771.
38. Jalilov, A. S.; Ruan, G.; Hwang, C.-C.; Schipper, D. E.; Tour, J. J.; Li, Y.; Fei, H.; Samuel, E. L. G.; Tour, J. M. Asphalt-Derived High Surface Area Activated Porous Carbons for Carbon Dioxide Capture. *ACS App. Mater. Interfases* **2015**, *7*, 1376-1382.
39. Srinivas, G.; Krungleviciute, V.; Guo, Z.-X.; Yildirim, T. Exceptional CO2 capture in a hierarchically porous carbon with simultaneous high surface area and pore volume. *Energy Environ. Sci.* **2014**, *7*, 335-342.
40. Ashourirad, B.; Sekizkardes, A. K.; Altarawneh, S.; El-Kaderi, H. M. Exceptional Gas Adsorption Properties by Nitrogen-Doped Porous Carbons Derived from Benzimidazole-Linked Polymers. *Chem. Mater.* **2015**, *27*, 1349-1358.
41. Adeniran, B.; Mokaya, R. Low temperature synthesized carbon nanotube superstructures with superior CO2 and hydrogen storage capacity. *J. Mater. Chem. A* **2015**, *3*, 5148-5161.
42. Himeno, S.; Komatsu, T.; Fujita, S. High-Pressure Adsorption Equilibria of Methane and Carbon Dioxide on Several Activated Carbons. *Journal of Chemical & Engineering Data* **2005**, *50*, 369-376.
43. Li, Y.; Ben, T.; Zhang, B.; Fu, Y.; Qiu, S. Ultrahigh Gas Storage both at Low and High Pressures in KOH-Activated Carbonized Porous Aromatic Frameworks. *Scientific Reports* **2013**, *3*, 2420.
44. Millward, A. R.; Yaghi, O. M. Metal−Organic Frameworks with Exceptionally High Capacity for Storage of Carbon Dioxide at Room Temperature. *J. Am. Chem. Soc.* **2005**, *127*, 17998-17999.

Table 1. Textural properties of porous carbons generated via conventional KOH chemical activation or melamine-mediated KOH chemical activation.

Hydrochar precursor	Sample code	Textural properties			
		S_{BET} [m^2 g^{-1}]	V_p [cm^3 g^{-1}] [a]	V_{micro} [cm^3 g^{-1}] [b]	V_{meso} [cm^3 g^{-1}] [c]
Starch	AA-0	3000	1.41	1.09	0.32 (23)
	AA-2M	3280	2.37	1.07	1.30 (55)
	AA-3M	3220	2.27	1.21	1.06 (47)
Cellulose	AC-0	3100	1.46	1.05	0.41 (28)
	AC-2M	3540	2.22	1.28	0.94 (42)
Sawdust	AS-0	2690	1.28	1.00	0.28 (22)
	AS-2M	3420	2.30	1.16	1.14 (50)
	AS-3M	2990	2.35	1.12	1.23 (52)

[a] Pore volume at P/P_o ~ 0.95. [b] Micropore volume determined by the D-R method. [c] Mesopore volume deduced by the difference between the pore volume and the micropore volume; the percentage of pore volume that corresponds to the mesopores is given in parenthesis.

Table 2. H_2 and CO_2 uptake at high pressure by porous carbon materials obtained by conventional KOH chemical activation and by melamine-mediated KOH chemical activation.

Hydrochar precursor	Sample code	H_2 uptake (wt%)[a]		CO_2 uptake (mmol g^{-1})[c]			
		Excess	Total[b]	1 bar	20 bar	40 bar	Working capacity (PSA system)[d]
Starch	AA-0	4.5	5.1 (5.6)	2.8	19.2	23.0	16.4 (20.2)
	AA-3M	5.0	6.4 (7.9)	2.5	20.4	30.1	17.9 (27.6)
Cellulose	AC-0	4.3	4.9 (5.3)	2.8	19.3	23.5	16.5 (20.7)
	AC-2M	5.3	6.7 (8.1)	2.3	20.8	29.8	18.5 (27.5)
Sawdust	AS-2M	5.3	6.8 (8.2)	2.2	20.5	30.6	18.3 (28.4)

[a] H_2 uptake at -196 ºC and 20 bar. [b] The estimated maximum hydrogen uptake capacity at -196 ºC derived from Langmuir simulation plots is provided in parenthesis. [c] CO_2 uptake at 25ºC. [d] Defined as the difference of equilibrium adsorption capacity at 20 bar (40 bar) and 1 bar.

Table 3. CO_2 uptake at high pressure for top-performing materials reported in the literature.

Material	CO_2 uptake @ 20 bar, 25 ºC [a] (mmol g^{-1})	Working capacity (PSA system)[d] (mmol g^{-1})	Reference
A*X*-*y*M (hydrochar-derived AC)	20-21 (30-31)	18-19 (27.5-28.4)	This work
VR5-4:1 (mesophase pitch-derived AC)	22 (31.8)	19.4 (29.2)	Ref. [17]
A-rNPC (asphalt-derived AC)	21.1 (26)[b]	17.1 (22)	Ref. [38]
HPC5b2-1100 (hierarchical porous carbons)	20.8 (27)[b]	17.1 (23.3)	Ref. [39]
CPC-700 (polymer-derived N-doped carbon)	21.4 (27.3)[c]	17.4 (23.3)	Ref. [40]
CN2800 (activated CNT superstructures)	19.5	16.7	Ref. [41]
Maxsorb (comercial AC)	19 (25.5)	16.9 (23.4)	Ref. [42]
PAF-1 (porous aromatic framework)	22.7 (30)	20.7 (28)	Ref. [43]
IRMOF-n MOF-177 (metal organic frameworks)	13.8-19.4 (14.7-22) 28.1 (34)	11.5-18.4 (12.4-21) 27.1 (33)	Ref. [44]

[a] Values in parenthesis correspond to a pressure of 40 bar. [b] Uptake at 30 bar. [c] Uptake at 35 bar. [d] Defined as the difference of equilibrium adsorption capacity at 20 and 1 bar. Values in parenthesis correspond to the difference of equilibrium adsorption capacity at 40 and 1 bar.

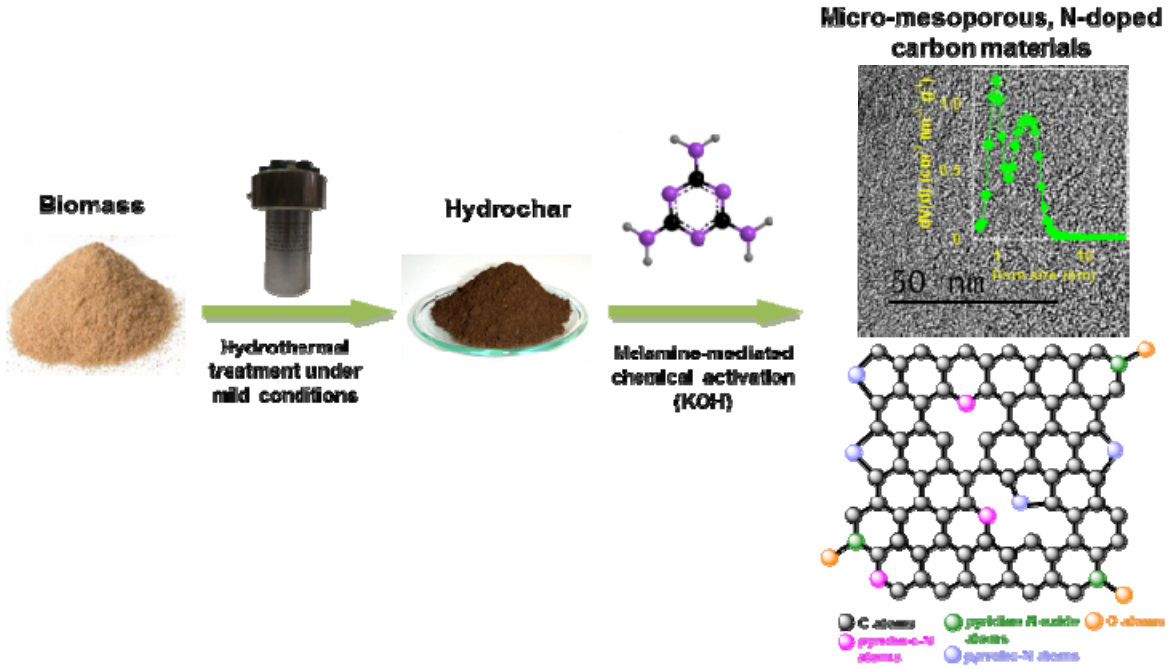

Scheme 1. Illustration of the synthesis methodology used for the production of highly porous micro-mesoporous, N-doped carbons from biomass-derived hydrochar.

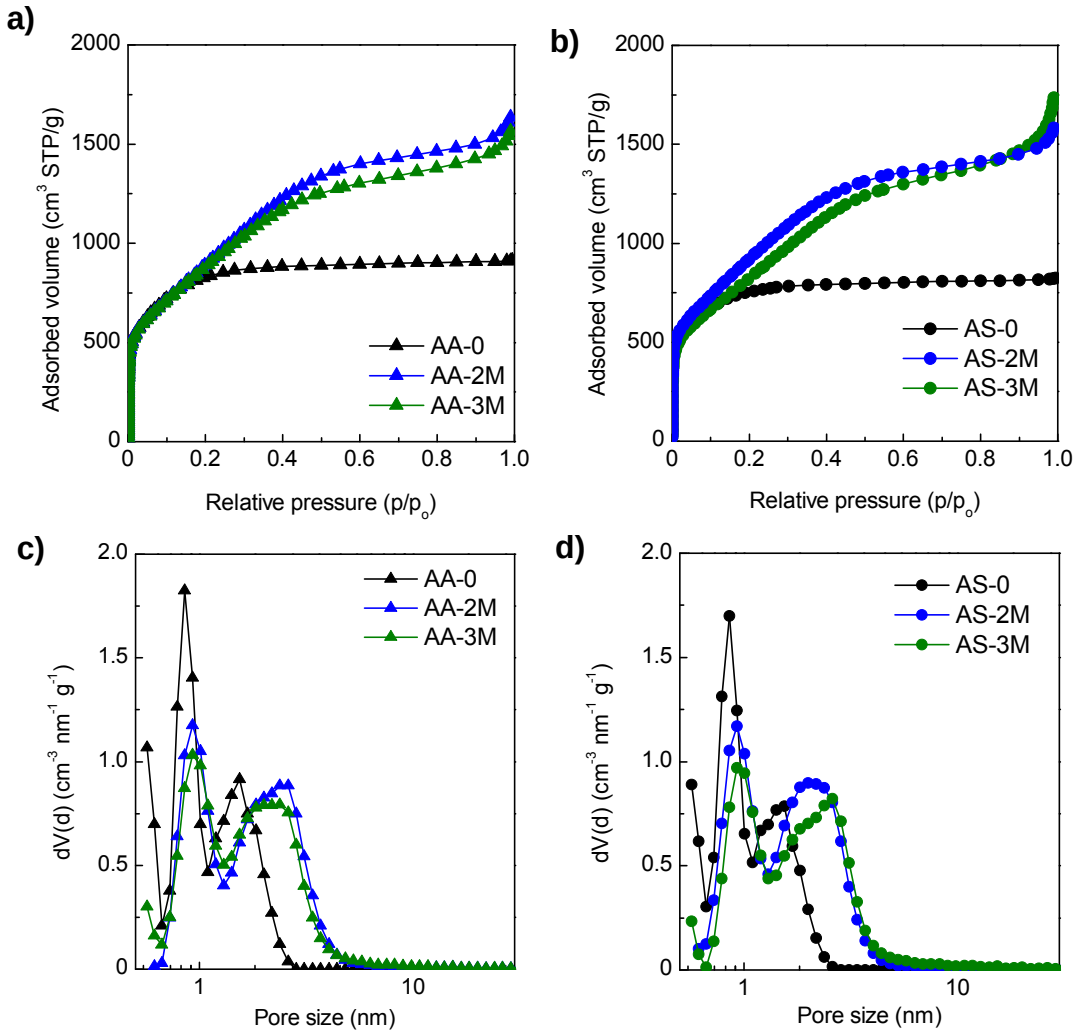

Figure 1. a, b) N_2 sorption isotherms and c, d) QSDFT PSDs curves of porous carbon materials produced in the absence and presence of melamine by using starch-and sawdust-derived hydrochars as carbon precursor.

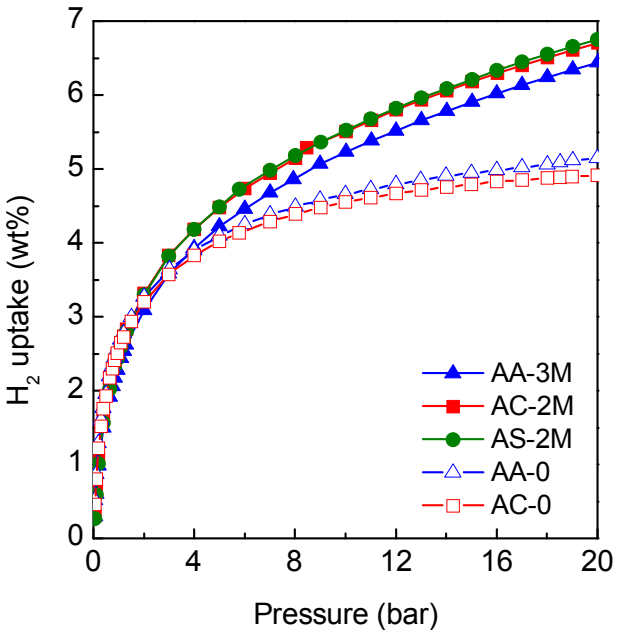

Figure 2. Total high pressure H_2 uptake isotherms obtained at -196 ºC for the hydrochar-based porous carbons.

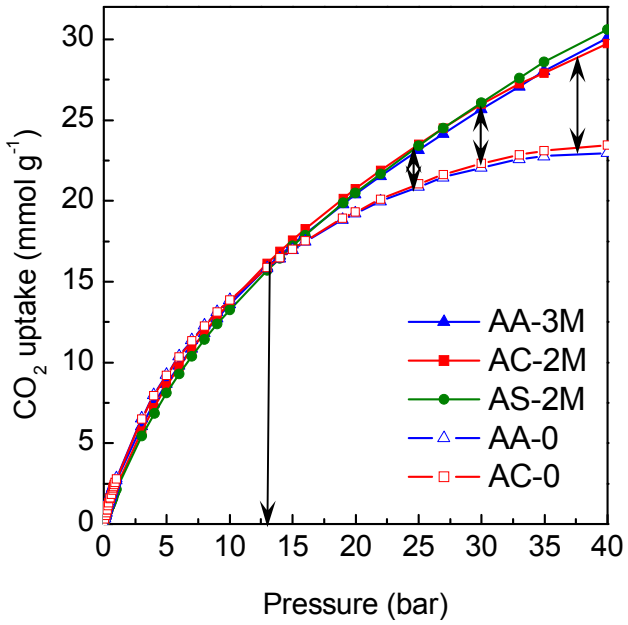

Figure 3. Total high pressure CO_2 uptake isotherms obtained at 25 ºC for the hydrochar-based porous carbons. The downwards arrow indicates the pressure at which the isotherms of the microporous and micro-mesoporous carbons intersect, whereas the up down arrows show the increase of the difference between the adsorption capacity of the microporous and micro-mesoporous carbons with the rise in pressure.